BCA-KMC Hybrid Simulation with Meta-Modeling for Hydrogen Dynamic Retention in Tungsten Material

A. M. Ito[1,2], S. Kato[3] and H. Nakamura[1,4]

[1]National Institute for Fusion Science, National Institutes of Natural Sciences, 322-6 Oroshi-cho, Toki 509-5292, Japan

[2]SOKENDAI, 322-6 Oroshi-cho, Toki 509-5292, Japan.

[3]Doshisha University, 1-3 Tatara Miyakodani, Kyotanabe-shi, Kyoto-fu 610-0394, Japan.

[4]Nagoya University, Furo-cho, Chikusa-ku, Nagoya 464-8603, Japan.

E-mail contact of main author: ito.atsushi@nifs.ac.jp

Abstract. To achieve the fuel balance and recycling in ITER and DEMO reactors, it is necessary to understand hydrogen behaviour in plasma facing materials. In this paper, we propose multi-scale meta-modelling simulation based on the hybrid simulation and automatic modelling as follows: (1)Binary Collision Approximation and Kinetic Monte-Carlo (BCA-KMC) hybrid simulation can simultaneously calculate the hydrogen isotope irradiation and the diffusion of hydrogen isotope atoms and vacancies beyond 1010 times the gap of their time scales. (2)A part of the KMC can treat the diffusion on grain boundary structures because the KMC model for migration paths is automatically constructed by Molecular Dynamics (MD). (3)The potential model for MD for the target material is also semi-automatically constructed by comparison with Density Functional Theory (DFT) calculation. The BCA-KMC can treat fluxes from laboratory experiment, 10^{20} $m^{-2}s^{-1}$, to ITER divertor environment, 10^{24} $m^{-2}s^{-1}$, and can reach the time scale of 10^{-2} s. The simulation result of the BCA-KMC signified that the retained hydrogen amount in the case of 10^{24} $m^{-2}s^{-1}$ is at least 10 times higher than that of 10^{22} $m^{-2}s^{-1}$.

1. Introduction

To understand plasma-material interaction (PWI) phenomena, it is important to research the dependence on the flux of plasma injection. The experimental fact that sputtering yield on carbon plasma facing material (PFM) decreases as the flux increases[1] was reported. Moreover, there are the phenomena induced when the fluence of plasma injection reaches threshold amount. The prime example is the tungsten fuzzy nanostructure induced by the helium plasma irradiation[2]. The tungsten fuzzy nanostructure is generated when the fluence of helium atoms reached about 10^{25} m^{-2}. Strictly speaking, the threshold to induce the tungsten fuzzy nanostructure is the retention amount of the helium atoms and its density distribution in materials. However, the measurement of the retention amount during plasma irradiation, which is called dynamic retention, is generally difficult in experiments. Therefore, the fluence of plasma injection has been often used as a measure instead of the retention amount. The dynamics retention of hydrogen isotope atoms is important also for the fuel balance in magnetic confinement fusion experimental devices/reactors and future ITER and DEMO reactors. Because the competition between the flux of plasma injection onto the materials and the diffusion speed of the injected impurity atoms in materials decides the dynamics retention, the flux dependence is key point to clarify the PWI phenomena.

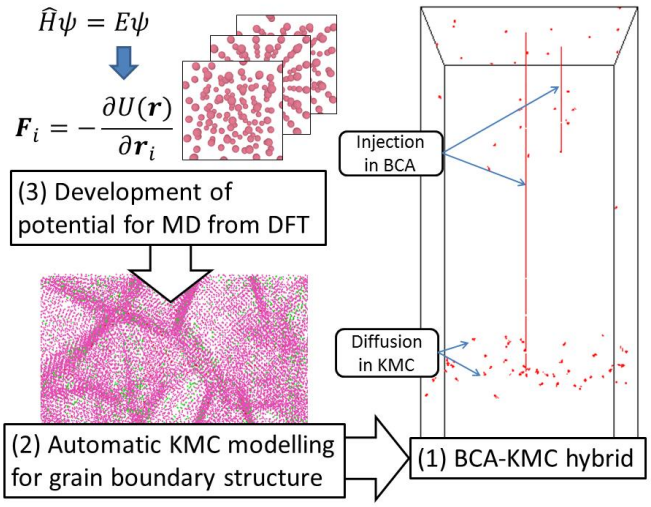

FIG. 1. The diagram of multi-scale meta-modelling (MSMM). The potential model for MD is generated by the downfolding method with DFT. The KMC model is automatically constructed by MD. Consequently, the BCA-KMC hybrid method simulates the dynamics retention during plasma irradiation.

In general, it is difficult to perform PWI experiments varying the injection flux in experimental devices. Therefore, experimental reports in terms of temperature or incident energy dependences occupy the existence experimental reports. The experimental report in terms of sputtering on carbon PFM noted above was the reclassification of the experimental data measured by different experimental devices. There is dispersion among different experimental devices. We should pay attention the extrapolation into high flux environment toward ITER and DEMO reactors, because the PWI phenomena are changed when the retention amount reaches threshold such as blistering, the fuzzy nanostructure, and so on.

To estimate the dynamics retention, the numerical simulation methods have been developed. Historically, binary collision approximation (BCA) and molecular dynamics (MD) has been used to treat the plasma irradiation process. However, these simulation methods are insufficient to estimate the dynamic retention. To begin with, BCA cannot treat continuous injection of plasma particles. Although MD can treat continuous injection of plasma particles, the calculation speed on current computers is too slow to achieve fluence corresponding to experimental fluence. In general, MD simulations employed the flux more than 10^5 times flux of experiments. The existing fastest MD simulation achieved the fluence of 10^{19} m^{-2} under the flux of 10^{25} $m^{-2}s^{-1}$. By comparison with experiments, the calculation speed of MD is insufficient more than 10^6 times. Our MD code GLIPS, the maximum calculation speed of MD is 10^8 step/day for 10^7 particles system on several ten thousand CPU cores of the current super computer systems, the Plasma Simulator in National Institute for Fusion Science and the HELIOS in IFERC-CSC under the Broader Approach collaboration between Euratom and Japan. If the number of CPU cores increases in future, the number of atoms treated in MD, that is space scale, will increases. However, the increase of the number of simulation steps in MD, that is time scale, is very difficult because the number of particles allocated per CPU core had already been smaller than several handled. Therefore, new simulation approach is necessary to achieve realistic flux and fluence corresponding to those of experiments. In particular, multiscale simulation approach[4] is recent trend in PWI simulation. One way to treat long-time scale PWI phenomena is coarse graining with translation to continuum modeling. Hydrogen dynamics retention was simulated by diffusion equation and rate equation on continuum density field[5]. The other way to treat long-time scale PWI

phenomena is hybrid simulation approach. For the tungsten fuzzy nanostructure formation, we developed the MD-MC hybrid simulation[6,7]. In the MD-MC hybrid simulation, the deformation of a tungsten material due to pressure from helium bubbles is simulated by MD, and long time diffusion of helium atoms in the tungsten material is quickly solved by Monte-Carlo (MC) simulation. The MD-MC hybrid simulation achieved the flux of 10^{22} $m^{-2}s^{-1}$ and the fluence of 10^{22} m^{-2}, and then the fuzzy nanostructure formation was reproduced. In the present paper, by utilizing experience of the development of hybrid method, we propose new hybrid simulation method connecting BCA and kinetic Monte-Carlo (KMC) to treat dynamics retention toward the condition of realistic flux and fluence corresponding to experiments.

Moreover, to research the competition between the flux of plasma injection and the diffusion speed of the impurity of the material, we should simulate not only the realistic flux and fluence but also the diffusion process of the impurity atoms in realistic material corresponding to experiments. The tungsten material used in experiments have grain boundary structures. The diffusion process of the impurity atoms strongly depends on grain boundary structures. The relationship of the macroscopic diffusivity measured from experiments and microscopic diffusion processes on grain boundary structures is not well clarified. Recently, the diffusion process of the impurity atoms on grain boundary has been investigated by using MD[8] and KMC[9] simulations. We aim to the simulation of the dynamic retention in materials with grain boundary structures directly taking into account injection processes in the BCA-KMC hybrid method. In general, the migration paths of the impurity atoms in KMC is constructed by using DFT calculations, whose calculation speed is slow. This is the bottleneck to expand the KMC model against arbitrary structured materials. In the present work, we propose multi-scale meta-modeling (MSMM) approach (See Fig. 1). In this approach, the migration paths in KMC is automatically and quickly constructed by using localized MD. In addition, the accuracy of the interaction potential model for MD is improved by using machine learning with database calculated by DFT.

2. Hybridization of Binary Collision Approximation and Kinetic Monte-Carlo

To estimate the competition of the injection flux of plasma ions and their diffusivity in a material, both the injection and the diffusion must be simultaneously simulated. Although MD can simulate both the injection and the diffusion, timescale reached by MD is too short to reproduce experimental real flux as mentioned above. Therefore, we have taken aim at calculation speed of simulation method. We have developed the hybrid method of binary collision approximation (BCA) and kinetic Monte-Carlo (KMC), which is here called BCA-KMC hybrid. In the BCA-KMC hybrid, the injection of plasma ions is simulated by BCA and the diffusion of impurity atoms in a material is simulated by KMC. The calculation speeds of both of BCA and KMC are very fast. Actually, BCA can achieve $10^{6\text{-}8}$ shots/day, and KMC can achieve 10^{11} steps/day.

The method to hybridize BCA and KMC is described. In KMC, physical phenomena are represented by the repeat of elemental events. Here, to treat diffusion process of the impurity atoms in a material, the elemental event is regarded as the migration of an impurity atom between local minimum energy sites. The event probability p_i of the i-th migration event is defined by

$$p_i = p_0(T)\exp(-\frac{\Delta E_i}{k_{\mathrm{B}}T})$$

where ΔE_i is the migration barrier energy on the i-th migration path, k_{B} is the Boltzmann constant, and T is material temperature. The prefactor $p_0(T)$ is a function of material temperature and can be determined from the diffusivity of the impurity atoms in a bulk

material having a pure lattice structure. The total event probability is given by $P_{\mathrm{mig}} = \sum_{i=1}^{N} p_i$ where N is the number of events. In each simulation step of KMC, the random number $r \subset [0, P_{\mathrm{mig}})$ is generated under the uniform distribution, and then one event k satisfying the condition

$$\sum_{i=1}^{k-1} p_i \leq r < \sum_{i=1}^{k} p_i$$

is chosen as occurrence event. According to the chosen k-th event, a impurity atom is moved along the k-th migration path. The time step is given by $\Delta t = -\frac{\ln u}{P}$ where $u \subset (0,1]$ is a random number generated under the uniform distribution. By this migration, the migration barrier energies for any atoms around the moved atom are changed. Therefore, before the next step, not only the event probability of the moved atom but also the event probabilities of atoms around the moved atom are recalculated. The total event probability P_{mig} is also recalculated. By repeating this routine, the diffusion process as the migrations of impurity atoms are simulated in KMC.

In general, the event in KMC is not only the migration of an atom. Any other elemental processes can be used as the event in KMC. The event probability of KMC is defined as the number of occurrence of the event per unit time and has the dimension of the inverse of time. In the BCA-KMC hybrid, an injection of a plasma ion is regarded as an event in KMC. The event probability of the injection is the number of ions injected onto the target surface per unit time. With the flux ϕ and the surface area S, the event probability of the injection is given by $p_{\mathrm{inj}} = \phi S$, the dimension of which is the inverse of time. The total event probability in the BCA-KMC hybrid is given by $P_{\mathrm{BCA-KMC}} = P_{\mathrm{mig}} + p_{\mathrm{inj}}$. The algorism for simulation step is same as the above way of simple KMC. When the event of migration is chosen, the target impurity atom is moved same as simple KMC, while when the event of injection is chosen, an ion is injected into the target surface from random position in the *x* and *y* directions by using BCA simulation. Even if the chosen event is the event of injection, the elapsed time in this step is determined by $\Delta t = -\frac{\ln u}{P}$.

In the event of injection by BCA, the injection target material has the common structure with that of the KMC part. The structure composed of the all atoms of tungsten material and the diffusing impurity atoms are shared between the BCA and KMC parts. The positions of the atoms in the target material are changed by every events of both the migration and the injection. If the injected ion stops in the target material due to energy loss, the injected ion becomes impurity atom and then it is put on the local minimum energy site which is the nearest site from the stop position in the BCA part. If atoms in the target material is sputtered out by collision with the injected ion, the sputtered atom is removed from the positions of atoms in the KMC part also. Since the positions of atoms are changed by the BCA part, the event probabilities in KMC part are recalculated before the next step. Thus, in the BCA-KMC hybrid, the KMC part and the BCA part have common structure of the target material at all time. The BCA part needs to treat the changed structures of the target material. Then, the ACAT[10] and the ACOCT[11] are the BCA codes to treat the amorphous structures and the lattice structures, respectively. In the previous work, the AC∀T[12] code to treat any structured targets based on the ACAT code. The BCA part in the BCA-KMC hybrid is based on these codes.

3. Multi-Scale Meta Modeling for Plasma Material Interaction

To simulate a realistic diffusion process, grain boundary structures should be treated in simulation. In the BCA-KMC hybrid simulation, the BCA part can treat arbitrary structured target materials based on the AC∀T code. To treat the diffusion processes of impurity atoms in arbitrary structured target material, all migration paths and migration barrier energies have to be prepared. We has developed the automatic KMC modeling[13]. By this method, all migration paths and migration barriers are automatically searched by using localized MD as follows.

First, local minimum energy sites for impurity atoms are searched in the target material as shown in Fig. 2(a) and (b). An impurity atom is put in one initial position. The localized MD varying the initial position is performed in the local region cutting off the impurity atom and its surrounding atoms only. The centre of the local region is the initial position of the impurity atom. The local region consists of two layers. The inside of the localized region is the movable region in which atoms are relaxed during the calculation of the localized MD, while the outside of the localized region is the fixed layer in which the atoms are fixed during the calculation of the localized MD. The size of the movable layer should be enough larger than the movement of atoms during the structure relaxation. The thickness of the fixed layer should be determined so that the forces acting on the atoms in the movable layer in the case of the localized MD equal to that in the case of full MD. In general, the thickness of the fixed layer is several integer multiple of the cut-off length in terms of multi-body potential models. Theoretical detail of the thickness of the fixed layer was stated in our previous work for the BCA-MD hybrid simulation [14], in which the MD part is similar to the localized MD. To find all local minimum energy sites, we required many localized MDs with the initial positions of impurity atoms which fill the whole of the simulation box. When found local minimum energy sites are overlapped, they are removed remaining one of them.

Next, migration paths connecting the local minimum energy sites and their migration barrier energies are estimated by using the localized MD also as shown in as shown in Fig. 2(a) and (c). The pair of local minimum energy sites whose distance is shorter than threshold length are picked up. The local region whose centre position is the centre of the pair sites. In the local region, the migration path connecting the pair sites are found by using the nudged elastic band (NEB) method [15] on the potential energy surface of the potential model for MD.

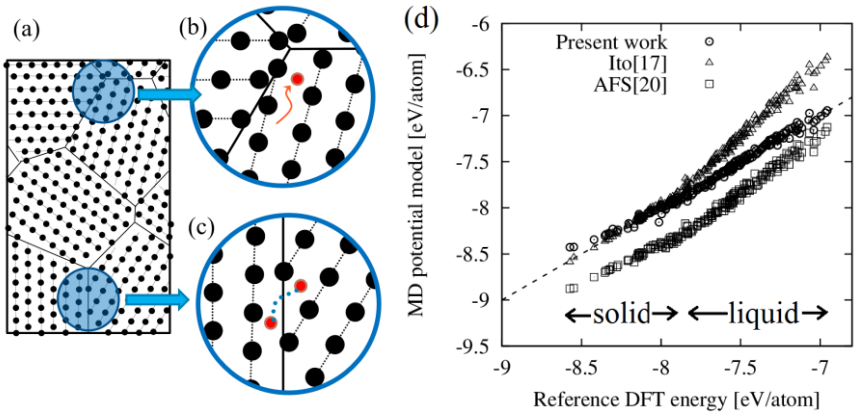

FIG. 2. Automatic KMC modelling by using localized MD. (a)Local regions are selected from the target material including a grain boundary structure. (b)The local minimum energy site is found by the structure relaxation of the structure with an impurity atom in the localized MD. (c)The migration path is found by the nudged elastic band calculation among the local minimum energy sites in the localized MD. (d)Optimized potential model for solid and liquid phases by using downfolding method.

Simultaneously, the migration barrier energy is also obtained. If the migration path has two local maximum energy points, the path is regarded as the path via the other local minimum energy site and then it is not counted. Thus, all migration paths and migration barrier energies are prepared.

The calculation of automatic KMC modelling are parallelized by the multi-program multi-data (MPMD) model [16] similar to the BCA-MD hybrid simulation [14]. The MPMD system consists of a master program and many working programs. The master program memorizes all atomic positions of the target material and lists up the local regions. The working programs perform the localized MD. As a result, all migration paths are found in short time.

The reliability of this automatic KMC modelling depends on the accuracy of the potential model for MD. In the MSMM, the potential model for MD is constructed by thermodynamic downfolding method [17,18]. The function form and its parameters of the potential model are optimized by comparison with the DFT calculations in many sample structures. The problem is how to prepare meaningful sample structures for the target material. Here, the sample structures are picked up from the multi-canonical ensemble MD, which is used for the simulation research on the structure change of protein folding in biological chemical physics [19]. Figure 2(d) shows the potential model optimized for both solid and liquid phases whose structures generated multi-canonical MD.

4. Result and Discussion

By using the BCA-KMC hybrid, the hydrogen plasma bombardment onto the tungsten material. The tungsten material has the body centered cubic (BCC) lattice structure. The (001) surface whose area is 63.3 nm $\times$ 63.3 nm faces vacuum region. The simulation box follows periodic boundary conditions in the *x-y* directions parallel to the surface. The incident energy of the hydrogen ions is 300 K. The incident direction is perpendicular to the surface. The incident position in the x-y direction is randomly determined under uniform distribution. The incident fluxes of 10^{20} $m^{-2}s^{-1}$, 10^{22} $m^{-2}s^{-1}$, and 10^{24} $m^{-2}s^{-1}$. The material temperatures are 300 K and 1000 K are simulated. Initially no hydrogen atom is retained in the material. Therefore, the initial event in BCA-KMC hybrid is the injection of the hydrogen ion by the BCA part.

The time evolution of the retention amount simulated by the BCA-KMC hybrid is shown in Fig. 3(a). The fluence of the hydrogen ion, which linearly increases with the elapsed time and but the magnitude of whose increases with flux, is adopted as the horizontal axis. Let us compare the two cases of the fluxes with 10^{22} $m^{-2}s^{-1}$ and 10^{24} $m^{-2}s^{-1}$ at 1000 K. In the case of low flux with 10^{22} $m^{-2}s^{-1}$, the retention amount is saturated, while in the case of high flux with 10^{24} $m^{-2}s^{-1}$, the retention amount continues to increases linearly. The saturation of the retention amount in the low flux case is caused by equilibrium between the insertion of the hydrogen atoms by plasma irradiation and its desorption from the surface via the diffusion in material. On the other hand, in the high case, the hydrogen retention is under the non-equilibrium state yet.

The difference of the flux causes also the difference of the space distribution of hydrogen atoms in a material. Fig. 3(b) shows the depth density distribution of retained hydrogen atoms for two cases of the fluxes with 10^{22} $m^{-2}s^{-1}$ and 10^{24} $m^{-2}s^{-1}$ at 1000 K where this data are snapshots at the fluence of 1.1×10^{18} m^{-2}. In the low flux case, the hydrogen atoms advance into the region deeper than 6×10^{3} Å from the surface. However, in the high flux case, the hydrogen atoms stay in the region shallower than 2×10^{3} Å from the surface. Moreover, the peak density of the retained hydrogen atoms in the high flux case is about 13 times higher than that in the low flux case. This reason is that the diffusivity of hydrogen atoms in a tungsten material is too slow to balance with the flux of 10^{24} $m^{-2}s^{-1}$. The difference if the

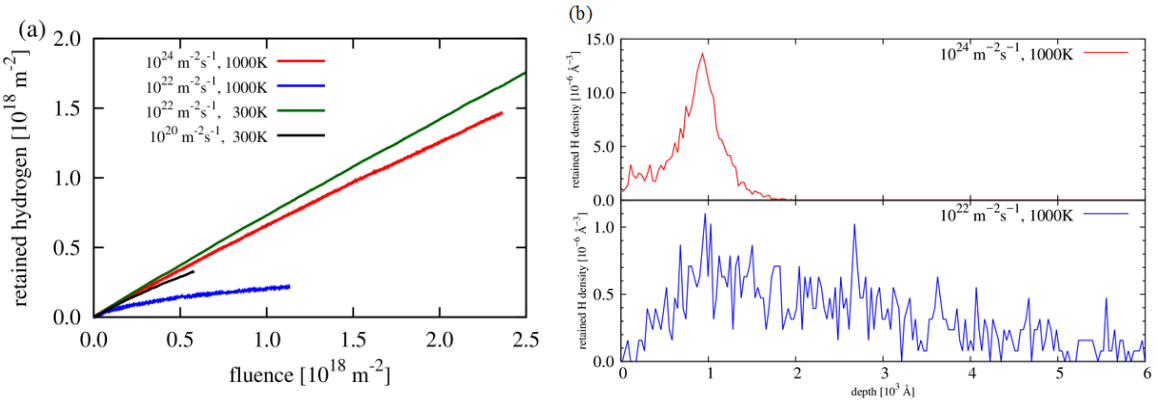

FIG. 3. (a)The hydrogen retention amount under the hydrogen ion bombardment as functions of fluence, which are calculated by the BCA-KMC hybrid. he incident energy of hydrogen ions is 300 eV. (b)The depth density distribution of retained hydrogen atoms at 1.1 × 10^{18} m^{-2} in the fluence and 300 eV in the incident energy of hydrogen ions.

depth density distribution warns us that the extrapolation of the retention amount to higher flux irradiation for the ITER and DEMO reactors should be carefully performed. If the density of the hydrogen atoms in material exceed threshold, the structure of the tungsten material is deformed such as the blistering.

The flux dependence is also confirmed in the comparison between the two cases of the fluxes with 10^{20} $m^{-2}s^{-1}$ and 10^{22} $m^{-2}s^{-1}$ at 300 K in Fig. 3(a). In general, as the flux increases, the retention amount at the same fluence becomes larger. Temperature dependence is also confirmed. The retention amount in the cases of the flux of 10^{22} $m^{-2}s^{-1}$ at 1000 K is saturated, while the retention amount at 300 K is not saturated in FIG 3(a). This reason is that the diffusivity of the impurity atoms decreases as the temperature decreases.

At the present moment, the BCA-KMC hybrid simulation has not calculate the case of the tungsten material with grain boundary structures. The development of method and code for the automatic KMC modelling had been completed. However, the potential model for tungsten and hydrogen system has not achieved sufficient accuracy. It was well known that there are larger differences among the existing potential models for tungsten and hydrogen system. We continue to develop MSMM approach. Ideally, in the MSMM, the simulation model is theoretically closed. Namely, almost all parameters for the simulation model can be determined from the MD with DFT level accuracy. In near future, we will report the grain boundary effect in the dynamic retention of hydrogen atoms by using BCA-KMC hybrid simulation with automatic KMC modelling.

5. Summary

The flux dependence is important to clarify PWI phenomena. To estimate the dynamic retention of hydrogen atoms in tungsten materials under, we developed the BCA-KMC hybrid method. The retention amount of hydrogen atoms were calculated. As a result, the flux dependence and the temperature dependence were shown as follows: the retention amount was saturated in the case of low flux with 10^{22} $m^{-2}s^{-1}$ at 1000 K, while the retention amounts were not saturated in the case of high flux with 10^{24} $m^{-2}s^{-1}$ or in the case at low temperature of 300 K. The peak of the depth density distribution of the retained hydrogen atoms in the case of 10^{24} $m^{-2}s^{-1}$ is greater than 10 times that of 10^{22} $m^{-2}s^{-1}$.

In future work, the dependence of the difference of the diffusivity due to the grain boundary structure in the tungsten material is researched. The automatic KMC modeling and the

potential development with downfolding and multi-canonical MD are powerful tool to expand the BCA-KMC hybrid simulation.

Acknowledgements

Authors thank Dr. Yasuhiro Oda for starting KMC simulation in our laboratory, and Dr. Seiki Saito for realizing the MPMD parallelization of localized MD in our previous works. This work was supported by KAKENHI (Nos. 15H05563 and 2524913) and by the National Institute for Fusion Science Collaboration Research programs (NIFS16KNSS068, NIFS14KNTS028, NIFS15KKGS158, NIFS16KNSS074, and NIFS16KNXN329). Numerical simulations were carried out by using the Plasma Simulator at NIFS and the HELIOS supercomputer system at the Computational Simulation Centre of International Fusion Energy Research Centre (IFERC-CSC), Aomori, Japan, under the Broader Approach collaboration between Euratom and Japan, implemented by Fusion for Energy and JAEA.

References

[1] ROTH, J., et al., Nucl. Fusion **44** (2004) L21.

[2] TAKAMURA, S., et al., Plasma Fusion Res. **1** (2006) 051.

[3] HAMMOND, K. D., et al., Euro. Phys. Lett. **110** (2015) 52002.

[4] WIRTH, B. D., J. Nucl. Mater. **463** (2015) 30–38.

[5] BLONDEL, S., et al, "Near-Surface Helium Segregation in Tungsten with the Xolotl Plasma-Surface Interactions Simulator", International Conference on Plasma Surface Interaction, May 30 – June 3, 2016, Roma, Italy, P2.13.

[6] ITO, A. M., et al., J. Nucl. Mater. **463** (2015) 109-115.

[7] ITO, A. M., et al., Nucl. Fusion **55** (2015) 073013.

[8] HU, L., et al., J. Appl. Phys. **115** (2014) 173512.

[9] ODA, T., ZHU, D., and WATANABE, Y., J. Nucl. Mater. **467** (2015) 439-447.

[10] YAMAMURA, Y. and MIZUNO. Y., IPPJ-AM-40, Inst. Plasma Phys., Nagoya University (1985).

[11] YAMAURA. Y., and TAKEUCHI, W., Nucl. Instrum. Methods Phys. Res., B**29** (1987) 461.

[12] TAKAYAMA, A., Jpn. J. Appl. Phys. **50** (2011) 01AB03.

[13] ITO, A. M., "Hydrogen Isotope Diffusion on Grain Boundary with Kinetic Monte-Carlo Model Automatically Constructed from Molecular Dynamics", International Conference on Plasma Surface Interaction, May 30 – June 3, 2016, Roma, Italy, P2.7.

[14] SAITO, S., et al., J. Nucl. Mater. **415** (2011) S208-S211.

[15] MILLS, G., and JÓNSSON, H., Phys. Rev. Lett. **72** (1994) 1124.

[16] TAKAYAMA, A., et al., J. Plasma Fusion Res. SERIES, **9** (2010) 604-609.

[17] ITO, A. M., et al., Phys. Scr. **T159** (2014) 014062.

[18] YOSHIMOTO, Y., J. Chem. Phys. **125** (2006) 184103.

[19] HANSMANN, U. H. E., Chem. Phys. Lett. **259** (1996) 321-330.

[20] ACKLAND, G. J. and THETFORD, R., Phil. Mag. A **56** (1987) 15–30.